Optical Selection Rule of Excitons in Gapped Chiral Fermion Systems

Xiaoou Zhang, Wen-Yu Shan, and Di Xiao
Department of Physics, Carnegie Mellon University, Pittsburgh, Pennsylvania 15213, USA

(Received 16 September 2017; published 15 February 2018)

We show that the exciton optical selection rule in gapped chiral fermion systems is governed by their winding number w, a topological quantity of the Bloch bands. Specifically, in a C_N-invariant chiral fermion system, the angular momentum of bright exciton states is given by $w \pm 1 + nN$ with n being an integer. We demonstrate our theory by proposing two chiral fermion systems capable of hosting dark s-like excitons: gapped surface states of a topological crystalline insulator with C_4 rotational symmetry and biased $3R$-stacked MoS_2 bilayers. In the latter case, we show that gating can be used to tune the s-like excitons from bright to dark by changing the winding number. Our theory thus provides a pathway to electrical control of optical transitions in two-dimensional material.

DOI: 10.1103/PhysRevLett.120.077401

Our understanding of optical absorption in semiconductors relies on two essential approximations [1]. The first is the effective mass approximation [2], in which the electron and the hole are considered as two particles moving with the effective masses of the conduction and valence bands, respectively. In the presence of the Coulomb interaction, the electron-hole pair will form a hydrogenlike bound state known as the exciton [3], which plays a crucial role in semiconductor optics. The second approximation is the electric dipole approximation. Within this approximation, the interband optical transition is usually understood in terms of the transition between atomic orbitals that make up the Bloch functions. Together, these two approximations yield the optical selection rule for excitons, as derived in a classic paper by Elliott [4]: If the band edge transition is dipole allowed, then only the s-like excitons are bright and the rest are dark. Despite its simplicity, this theory is quite versatile and can be further generalized to include complications such as band degeneracy, anisotropy, and spin-orbit interaction.

However, the validity of the above theory has been recently challenged in a new class of materials called gapped chiral fermion (CF) systems. Examples include gapped topological surface states [5], biased bilayer graphene [6,7], and monolayers of group-VI transition metal dichalcogenides such as MoS_2 [8–10]. It has been shown that in these systems the effective mass approximation must be modified to include the Berry phase [11] carried by the CFs to give a proper account of the exciton energy spectrum [12,13]. At the same time, anomalous exciton optical selection rules have also been found in these systems. For example, it has been shown that both the s-like and d-like excitons are bright in monolayer MoS_2, and their optical transitions have opposite circular polarization [14], while in biased bilayer graphene it is the p-like excitons that are bright [6]. These results suggest that a new exciton optical selection rule must be established in gapped CF systems.

In this Letter, we show that the exciton optical selection rule in gapped CF systems is governed by their winding number w [see Eq. (1) below], a topological property of the Bloch bands [15,16]. Specifically, we find that the bright excitons in an isotropic CF system have angular momentum $m = w \pm 1$. When the full rotational symmetry is reduced to discrete C_N symmetry by the crystal field effect, the allowed angular momentum of bright excitons expands to $m = w \pm 1 + nN$, where n is an integer. Our theory thus gives a unified view of the optical selection rule previously found in various gapped CF systems [5,6,14]. To further demonstrate our theory, we propose two gapped CF systems capable of hosting dark s-like excitons. The first is gapped surface states of a topological crystalline insulator with C_4 symmetry. The second is $3R$-stacked MoS_2 bilayers. In the latter case, we show that gating can be used to tune the s-like exciton from bright to dark by changing the winding number. The value of the gate voltage to realize such a dark-bright transition is within experimental reach. Our study, together with the previous result of the Berry phase effect on the exciton spectrum [12,13], provides a basic description of the electronic structure of excitons in gapped CF systems.

We begin with the $\boldsymbol{k} \cdot \boldsymbol{p}$ Hamiltonian for an isotropic two-dimensional CF model with an integer winding number w:

$$H_0 = \begin{pmatrix} \Delta & \alpha(|\boldsymbol{k}|)e^{iw\phi_{\boldsymbol{k}}} \\ \alpha(|\boldsymbol{k}|)e^{-iw\phi_{\boldsymbol{k}}} & -\Delta \end{pmatrix}, \tag{1}$$

where 2Δ is the energy gap and $\phi_{\boldsymbol{k}} = \tan^{-1}(k_y/k_x)$. This Hamiltonian describes a wide range of material systems. For example, both gapped topological surface states [5] and monolayer MoS_2 [8] have $\alpha(|\boldsymbol{k}|) \propto |\boldsymbol{k}|$ with the winding

number $w = 1$, and biased bilayer graphene has $\alpha(|\boldsymbol{k}|) \propto |\boldsymbol{k}|^2$ with $w = 2$ [17]. In fact, in graphene multilayers, w can be made arbitrary integral values [18]. We note that this model also includes the special case of a zero winding number, even though it cannot be called a chiral fermion anymore. The energy dispersion of this model is given by $\varepsilon_{c,v} = \pm\varepsilon_{\boldsymbol{k}} = \pm\sqrt{\Delta^2 + \alpha^2(|\boldsymbol{k}|)}$ with the corresponding eigenstates

$$|c\boldsymbol{k}\rangle = \begin{pmatrix} \cos\frac{\theta_k}{2} \\ \sin\frac{\theta_k}{2} e^{-iw\phi_k} \end{pmatrix}, \qquad |v\boldsymbol{k}\rangle = \begin{pmatrix} \sin\frac{\theta_k}{2} e^{iw\phi_k} \\ -\cos\frac{\theta_k}{2} \end{pmatrix}, \quad (2)$$

where $\theta_k = \cos^{-1}(\Delta/\epsilon_{\boldsymbol{k}})$. The wave functions have a U(1) gauge freedom. Here we fix the gauge by demanding that both $|c\boldsymbol{k}\rangle$ and $|v\boldsymbol{k}\rangle$ have no singularity at the band edge ($\boldsymbol{k} = 0$). Under this gauge choice, the labeling of excitons by their angular momenta returns to that of the hydrogenic model in the large gap limit [12].

An exciton in a general two-band model can be written as a linear combination of electron-hole pairs:

$$|\Psi(\boldsymbol{q})\rangle = \sum_{\boldsymbol{k}} f_{\boldsymbol{q}}(\boldsymbol{k}) a^\dagger_{c\boldsymbol{k}+\boldsymbol{q}} a_{v\boldsymbol{k}} |\Omega\rangle. \quad (3)$$

Here $|\Omega\rangle$ is the semiconductor ground state with the valence band filled and the conduction band empty, and $a^\dagger_{c\boldsymbol{k}+\boldsymbol{q}}$ ($a_{v\boldsymbol{k}}$) creates an electron (hole) in the conduction (valence) band. The coefficient $f_{\boldsymbol{q}}(\boldsymbol{k})$ is the exciton envelope function, where $\boldsymbol{q}$ and $\boldsymbol{k}$ are the center-of-mass and relative momentum of the electron-hole pair, respectively. For photoexcited excitons, the center-of-mass momentum $\boldsymbol{q}$ is negligible, which will be set to zero and omitted hereafter. In the isotropic model, the angular momentum m is a good quantum number; thus, the envelope functions have the following form:

$$f_m(\boldsymbol{k}) = \tilde{f}_m(|\boldsymbol{k}|) e^{im\phi_k}. \quad (4)$$

Finally, the oscillator strength of an exciton with angular momentum m under circular polarization is given by

$$O_m = \frac{1}{\mu E^{\mathrm{ex}}_m} \sum_{\eta=\pm} \left| \int d\boldsymbol{k} \tilde{f}_m(|\boldsymbol{k}|) e^{im\phi_k} v_\eta(\boldsymbol{k}) \right|^2, \quad (5)$$

where $v_\eta(\boldsymbol{k}) = \langle v\boldsymbol{k}|\hat{v}_\eta|c\boldsymbol{k}\rangle$ is the interband matrix element of the velocity operator $\hat{v}_\eta = \hat{v}_x + i\eta\hat{v}_y$ with $\hat{v}_{x,y} = \partial H_0/\partial k_{x,y}$, E^{ex}_m is the exciton energy, and μ is the reduced mass.

It should be pointed out that there are generally two contributions to the velocity matrix element: One is from the electron hopping between lattice sites, and the other from the dipole transition between localized orbitals [19]. Here we consider only the former contribution while neglecting the latter. This is justified for the systems considered in this Letter. In MoS_2, the conduction and valence band edges are mainly formed by the Mo d orbitals, with slight mixing from the S p orbitals [20]. There is no dipole transition between the even-parity d orbitals, and transitions between d and p orbitals are negligible. Similarly, in gapped graphene systems, the atomic orbitals involved are carbon p_z orbitals, and optical transitions among them are dipole forbidden.

Near the band edge, the angular dependence of the velocity matrix element is given by [21]

$$\langle v\boldsymbol{k}|\hat{v}_\pm|c\boldsymbol{k}\rangle \propto e^{-i(w\mp1)\phi_k}. \quad (6)$$

It then follows from Eq. (5) that after angular average only exciton states with $m = w \pm 1$ have a nonzero oscillator strength. In addition, optical transitions to these two angular momentum states always have opposite circular polarization. We emphasize that it is the $\boldsymbol{k}$-space phase winding of the velocity matrix element, a feature not available in the atomic transition picture, that determines the exciton optical selection rule of gapped CF systems.

Although both $w + 1$ and $w - 1$ states are bright, their oscillator strength can be quite different. For simplicity, we assume $\alpha(|\boldsymbol{k}|) = \alpha|\boldsymbol{k}|^w$. The velocity matrix elements take the form

$$\begin{aligned} \langle v\boldsymbol{k}|\hat{v}_+|c\boldsymbol{k}\rangle &= -2\alpha w \cos^2\frac{\theta_k}{2} k^{w-1} e^{-i(w-1)\phi_k}, \\ \langle v\boldsymbol{k}|\hat{v}_-|c\boldsymbol{k}\rangle &= 2\alpha w \sin^2\frac{\theta_k}{2} k^{w-1} e^{-i(w+1)\phi_k}. \end{aligned} \quad (7)$$

In the large band gap limit, i.e., $\Delta \gg \alpha k_B^w$, where k_B is the inverse of the exciton Bohr radius, we have $\cos(\theta_{k_B}/2) \gg \sin(\theta_{k_B}/2)$. In this case, the $m = w - 1$ exciton states are much brighter than the $m = w + 1$ states.

So far, we have considered only the isotropic case. However, in a crystalline environment, the C_∞ symmetry is reduced to C_N by the crystal field effect, which will modify the optical selection rule. The modifications come from two places. First, the exciton state with angular momentum m is mixed with those with angular momentum $m + nN$:

$$f_m(\boldsymbol{k}) \to \tilde{f}_m(|\boldsymbol{k}|) e^{im\phi_k} + \sum_{n\neq0} c_n \tilde{f}_{m+nN}(|\boldsymbol{k}|) e^{i(m+nN)\phi_k}, \quad (8)$$

where n is an integer and c_n is the coefficient for each angular momentum channel, whose form has been derived in Ref. [21]. Second, the velocity matrix element is also expanded into a series of angular momentum channels [21]:

$$\langle v\boldsymbol{k}|\hat{v}_\pm|c\boldsymbol{k}\rangle = \sum_n v_n e^{-i(w\mp1+nN)\phi_k}. \quad (9)$$

According to Eq. (5), the exciton selection rule now reads

$$m = w \pm 1 + nN. \quad (10)$$

This is a reflection of the fact that in a C_N-invariant system the angular momentum is defined only modulo N [22]. Finally, we note that the optical transitions to the m and $(m + nN)$ states have the same circular polarization.

Now we examine our theory in the two previously studied systems. The first one is monolayer MoS_2 with

winding number $w = 1$. According to our theory, the s- and d-like excitons should be bright with opposite circular polarizations when the crystal field effect is ignored, and the s state should be much brighter than the d state due to the relatively large band gap in MoS_2 ($\alpha k_B/\Delta \sim 0.1$) [8,12]. If we turn on the crystal field, the symmetry is reduced from C_∞ to C_3. In this case, the p-like state with $m = -1$, which is dark in the isotropic model, becomes bright and has the same polarization as the d-like excitons with $m = 2$. This result agrees with the direct calculation in a recent study [14].

The second example is the biased bilayer graphene [6], which is described by the following effective Hamiltonian [17]:

$$H_{\mathrm{BLG}} = \begin{pmatrix} \Delta & \alpha k_+^2 \\ \alpha k_-^2 & -\Delta \end{pmatrix} + 3\gamma_3 \begin{pmatrix} 0 & k_- \\ k_+ & 0 \end{pmatrix}, \quad (11)$$

where $k_\pm = k_x \pm i k_y$ and γ_3 is the interlayer hopping amplitude. The first term in H_{BLG} describes an isotropic CF model with winding number $w = 2$. This term alone would give rise to dark s states, since only the $m = 1$ and $m = 3$ states are bright. However, in the presence of the γ_3 term, which reduces the C_∞ symmetry to C_3, the optical transitions to s-like states are turned on and have opposite circular polarization compared to the p-like states. Similarly, the $m = -2$ states also become bright (see Fig. 1).

To estimate the crystal field effect, we have carried out a perturbative calculation by treating γ_3 as a small quantity in the large band gap limit [21]. We find that the modification to the exciton envelope function is a higher-order contribution, and the main effect of the crystal field comes from its modification to the velocity matrix element, which is proportional to γ_3. Accordingly, the ratio of the oscillator strength between the s and p states should be proportional to $9\gamma_3^2/(2\alpha|k_B|)^2$ [21]. According to Ref. [6], the k-space radius of the exciton envelope function is $k_B \sim 0.02$ Å^{-1}, which gives $9\gamma_3^2/(2\alpha|k_B|)^2 \sim 0.02$. Note that, from a pure group theory point of view, we can also come to the conclusion that the s-like excitons are bright. In contrast, our theory provides a quantitative estimation of the brightness of the s state.

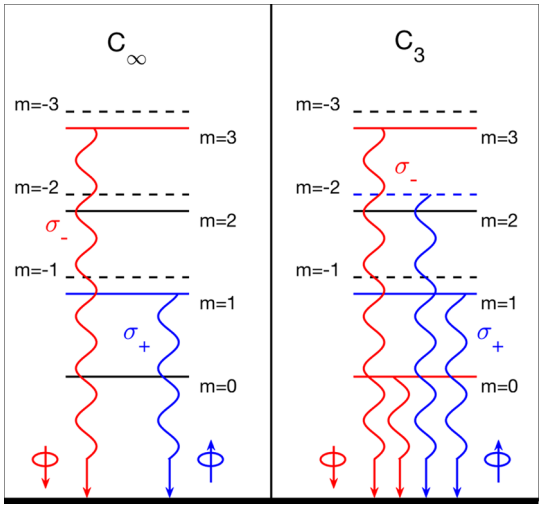

FIG. 1. The exciton optical selection rule of the $w = 2$ chiral fermion model when the symmetry is reduced from (a) C_∞ to (b) C_3. The black lines indicate dark states, and the red (blue) lines are bright states with σ_- (σ_+) polarization. The solid lines represent positive angular momenta, and the dashed lines represent negative angular momenta.

The fact that it is the C_3 symmetry that turns the s-like excitons bright in a $w = 2$ CF system suggests that, by switching to a different rotational symmetry, the s states can remain dark. One such system is the gapped surface states of a topological crystalline insulator with a possible C_4 rotational symmetry [23]. The Hamiltonian for the surface states in such a system is given by

$$H_{\mathrm{TCI}} = a_1 \begin{pmatrix} V_z & k_+^2 \\ k_-^2 & -V_z \end{pmatrix} + a_2 \begin{pmatrix} V_z & k_-^2 \\ k_+^2 & -V_z \end{pmatrix}, \quad (12)$$

where V_z is the gap opened by a time-reversal-breaking perturbation [21,23]. We can see that this model is a mixture of CFs with $w = \pm 2$. The simultaneous existence of both winding numbers reduces the rotational symmetry to C_4, and the s states remain dark.

Apart from varying the symmetry group, we can also obtain dark s states by switching to a different winding number while keeping the C_3 symmetry. For this purpose, let us consider $3R$-stacked MoS_2 bilayers. In the $3R$-stacked bilayer structure, the top layer is shifted relative to the bottom layer along the honeycomb armchair edge, as shown in Fig. 2. Neglecting the spin degree of freedom, the effective Hamiltonian at one of the corners of the hexagonal Brillouin zone is given by [21]

$$H_{3\mathrm{R}} = \begin{pmatrix} \Delta_I + V_g & v_0 k_- & 0 & 0 \\ v_0 k_+ & -\Delta_I + V_g & \gamma_1 & 0 \\ 0 & \gamma_1 & \Delta_I - V_g & v_0 k_- \\ 0 & 0 & v_0 k_+ & -\Delta_I - V_g \end{pmatrix}, \quad (13)$$

where Δ_I is the gap opened by the broken inversion symmetry in each monolayer, V_g is the out of plane gate voltage, and v_0 and γ_1 are the intralayer and interlayer hopping coefficients, respectively. We have kept only the isotropic part of the Hamiltonian, which is sufficient to demonstrate the essential physics. An interesting feature of this system is that by varying V_g one can switch the band order within the conduction and valence bands (see Fig. 3). If we assume that Δ_I is large compared with the interlayer hopping constant γ_1, the critical value of the gate voltage

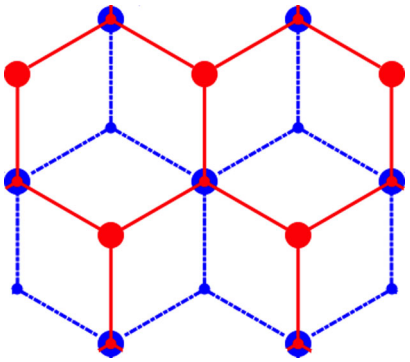

FIG. 2. Top view of $3R$-stacked MoS_2 bilayers. The large dots are Mo atoms, and the small ones are S atoms. Red (blue) dots refer to the atoms in layer 1 (2).

V_{gc} at the band crossing point is approximately $\gamma_1^2/2\Delta_I$. For intralayer band gap $\Delta_I \approx 0.8$ eV and interlayer hopping $\gamma_1 \approx 0.05$ eV [24], the required V_{gc} is about 1.5 meV, which is not difficult to achieve in an experiment [25].

The ability to switch the bands is important, because the winding number is a topological quantity; it can be changed via band crossing only if the rotational symmetry is kept invariant. To find the winding number before and after the band crossing, we downfold the Hamiltonian (13) to project out the higher conduction band and the lower valence band [26]. Before the band crossing, i.e., $V_g < V_{gc}$, the downfolded Hamiltonian reads

$$H_{\text{before}} = \begin{pmatrix} \Delta_I + V_g & \frac{v_0^2\gamma_1}{4\Delta_I V_g} k_-^2 \\ \frac{v_0^2\gamma_1}{4\Delta_I V_g} k_+^2 & -\Delta_I - V_g \end{pmatrix}. \tag{14}$$

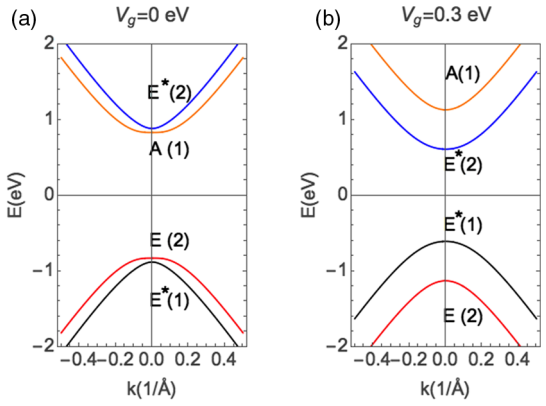

FIG. 3. Band structure of a biased $3R$-MoS_2 bilayer at (a) $V_g = 0$ eV and (b) $V_g = 0.3$ eV. Bands with different colors belong to different irreducible representations of the C_3 group and layer number (1,2). The parameters used are $\Delta_I = 0.83$ eV and $v_0 = 3.5$ eV Å [24]. We used a large interlayer hopping term, $\gamma_1 = 0.3$ eV, to make the band separation visible.

We can see that the winding number $w = 2$, similar to the biased bilayer graphene. This is not surprising, because each monolayer MoS_2 carries winding number $w = 1$, and, in the $3R$-stacking, one can simply add the winding numbers together [27]. In this case, the s-like exciton is bright in the presence of the C_3 symmetry. After the band crossing, i.e., $V_g > V_{gc}$, the 2×2 Hamiltonian is

$$H_{\text{after}} = \begin{pmatrix} -\sqrt{\gamma_1^2 + (\Delta_I - V_g)^2} & -\frac{v_0^2\gamma_1(\Delta_I + V_g)}{4(\Delta_I - V_g)\Delta_I V_g} k^2 \\ -\frac{v_0^2\gamma_1(\Delta_I + V_g)}{4(\Delta_I - V_g)\Delta_I V_g} k^2 & \sqrt{\gamma_1^2 + (\Delta_I - V_g)^2} \end{pmatrix}. \tag{15}$$

Clearly, the winding number is changed to $w = 0$. Hence, $m = \pm 1$ states become bright. Turning on C_3 symmetry makes $m = \pm 1, \pm 4, \ldots$ states bright, but the s states remain dark.

Up to now, we have omitted the valley degree of freedom, which exists in most chiral fermion systems such as graphene and MoS_2 monolayers. Different valleys carry an opposite winding number as a result of the time-reversal symmetry. The corresponding optical transitions therefore have opposite circular polarization. However, intervalley coupling of exciton states via the same circularly polarized light is unlikely, since the bright exciton states in the two valleys usually have different energies (for the same circular polarization).

In conclusion, we have established a new optical selection rule of excitons in a gapped CF system. We found that the angular momentum of bright excitons is $w \pm 1$ in the isotropic cases, and the circular polarizations of these two states are opposite. When the crystal field effect is taken into account, the optically bright excitons have angular momentum $(w \pm 1) + nN$ if the system has N-fold rotational symmetry. We showed that, by proper combinations of the winding number and rotational symmetry, one can engineer dark s states in CF systems. The occurrence of dark excitons has already been under intense experimental investigation [28–31]. Such a dark exciton has a prolonged lifetime [32] and can be utilized to realize exciton condensation [33–35] and implement quantum information protocols [36,37].

This work is supported by the Department of Energy, Basic Energy Sciences, Grant No. DE-SC0012509. D. X. also acknowledges support from a Research Corporation for Science Advancement Cottrell Scholar Award.

X. Z. and W. S. contributed equally to this work.

Note added.—Recently, we have become aware of a recent paper, Ref. [38], which also studied the exciton optical selection rule in graphene systems.

[1] P. Y. Yu and M. Cardona, *Fundamentals of Semiconductors*, 4th ed. (Springer-Verlag, Berlin, 2010).
[2] J. M. Luttinger and W. Kohn, Phys. Rev. **97**, 869 (1955).
[3] G. H. Wannier, Phys. Rev. **52**, 191 (1937).
[4] R. J. Elliott, Phys. Rev. **108**, 1384 (1957).
[5] I. Garate and M. Franz, Phys. Rev. B **84**, 045403 (2011).
[6] C.-H. Park and S. G. Louie, Nano Lett. **10**, 426 (2010).
[7] L. Ju, L. Wang, T. Cao, T. Taniguchi, K. Watanabe, S. G. Louie, F. Rana, J. Park, J. Hone, F. Wang, and P. L. McEuen, Science **358**, 907 (2017).
[8] D. Xiao, G.-B. Liu, W. Feng, X. Xu, and W. Yao, Phys. Rev. Lett. **108**, 196802 (2012).
[9] M. M. Glazov, L. E. Golub, G. Wang, X. Marie, T. Amand, and B. Urbaszek, Phys. Rev. B **95**, 035311 (2017).
[10] G. Wang, A. Chernikov, M. M. Glazov, T. F. Heinz, X. Marie, T. Amand, and B. Urbaszek, arXiv:1707.05863.
[11] D. Xiao, M.-C. Chang, and Q. Niu, Rev. Mod. Phys. **82**, 1959 (2010).
[12] J. Zhou, W.-Y. Shan, W. Yao, and D. Xiao, Phys. Rev. Lett. **115**, 166803 (2015).
[13] A. Srivastava and A. Imamoğlu, Phys. Rev. Lett. **115**, 166802 (2015).
[14] P. Gong, H. Yu, Y. Wang, and W. Yao, Phys. Rev. B **95**, 125420 (2017).
[15] J. N. Fuchs, F. Piéchon, M. O. Goerbig, and G. Montambaux, Eur. Phys. J. B **77**, 351 (2010).
[16] Y. Gao and Q. Niu, Proc. Natl. Acad. Sci. U.S.A. **114**, 7295 (2017).
[17] E. McCann and V. I. Fal'ko, Phys. Rev. Lett. **96**, 086805 (2006).
[18] H. Min and A. H. MacDonald, Phys. Rev. B **77**, 155416 (2008).
[19] T. G. Pedersen, K. Pedersen, and T. B. Kriestensen, Phys. Rev. B **63**, 201101 (2001).
[20] G.-B. Liu, W.-Y. Shan, Y. Yao, W. Yao, and D. Xiao, Phys. Rev. B **88**, 085433 (2013).
[21] See Supplemental Material at http://link.aps.org/supplemental/10.1103/PhysRevLett.120.077401 for detailed derivations of the velocity matrix elements, the optical selection rule with the crystal field effect, and the effective Hamiltonians used in the main text.
[22] W. Yao, D. Xiao, and Q. Niu, Phys. Rev. B **77**, 235406 (2008).
[23] L. Fu, Phys. Rev. Lett. **106**, 106802 (2011).
[24] These data are the hopping constants for 2H-stacked MoS_2 bilayers [25], as an estimate for 3*R* stacking.
[25] S. Wu, J. S. Ross, G.-B. Liu, G. Aivazian, A. Jones, Z. Fei, W. Zhu, D. Xiao, W. Yao, D. Cobden, and X. Xu, Nat. Phys. **9**, 149 (2013).
[26] R. Winkler, *Spin-Orbit Coupling Effects in Two-Dimensional Electron and Hole Systems* (Springer, New York, 2003).
[27] H. Min, R. Bistritzer, J.-J. Su, and A. H. MacDonald, Phys. Rev. B **78**, 121401 (2008).
[28] Z. Ye, T. Cao, K. O'Brien, H. Zhu, X. Yin, Y. Wang, S. G. Louie, and X. Zhang, Nature (London) **513**, 214 (2014).
[29] X.-X. Zhang, Y. You, Shu Yang Frank Zhao, and T. F. Heinz, Phys. Rev. Lett. **115**, 257403 (2015).
[30] X.-X. Zhang, T. Cao, Z. Lu, Y.-C. Lin, F. Zhang, Y. Wang, Z. Li, J. C. Hone, J. A. Robinson, D. Smirnov, S. G. Louie, and T. F. Heinz, Nat. Nanotechnol. **12**, 883 (2017).
[31] B. Scharf, G. Xu, A. Matos-Abiague, and I. Žutić, Phys. Rev. Lett. **119**, 127403 (2017).
[32] C. Robert, T. Amand, F. Cadiz, D. Lagarde, E. Courtade, M. Manca, T. Taniguchi, K. Watanabe, B. Urbaszek, and X. Marie, Phys. Rev. B **96**, 155423 (2017).
[33] M. Combescot, O. Betbeder-Matibet, and R. Combescot, Phys. Rev. Lett. **99**, 176403 (2007).
[34] R. Anankine, M. Beian, S. Dang, M. Alloing, E. Cambril, K. Merghem, C. G. Carbonell, A. Lemaitre, and F. Dubin, Phys. Rev. Lett. **118**, 127402 (2017).
[35] K. H. Lee, C. Lee, H. Min, and S. B. Chung, arXiv:1710.00841.
[36] E. Poem, Y. Kodriano, C. Tradonsky, N. H. Lindner, B. D. Gerardot, P. M. Petroff, and D. Gershoni, Nat. Phys. **6**, 993 (2010).
[37] I. Schwartz, D. Cogan, E. R. Schmidgall, Y. Don, L. Gantz, O. Kenneth, N. H. Lindner, and D. Gershoni, Science **354**, 434 (2016).
[38] T. Cao, M. Wu, and S. G. Louie, arXiv:1708.02227 [Phys. Rev. Lett. (to be published)].